euronoise 2021
25th to 27th of October
Madeira, Portugal - online

Acoustic absorption of porous concrete – normal incidence vs diffuse field conditions

Laura Lourenço de Sousa[1], Luís Pereira[1], Denilson Ramos[1], Luís Godinho[1], Paulo Amado Mendes[1]

[1] University of Coimbra, ISISE, Department of Civil Engineering, Coimbra, Portugal
lrldsousa@uc.pt, lfmpereira@uc.pt, dtramos@student.dec.uc.pt, lgodinho@dec.uc.pt, pamendes@dec.uc.pt

Abstract

Porous solutions for sound absorption purposes have been the target of several studies. In this work, the acoustic absorption behaviour of concrete-based porous material was determined both experimentally and theoretically. The aggregates used in the concrete mixtures were one expanded clay. Tests were carried out for normal sound incidence in an impedance tube and diffuse field conditions, in a reverberation room, in order to obtain the samples sound absorption coefficient. Analytical methodologies were used, including the analytical equations proposed by ISO 10534-2 and London, to estimate diffuse field absorption from normal incidence results. Significant differences were registered between the theoretical estimations of diffuse field absorption and the measured results in reverberant room.

Keywords: Porous concrete, Sound absorption coefficient, Normal sound incidence, Diffuse field conditions.

1 Introduction

Porous materials are wildely used to improve the sound environment conditions through their sound absorption properties. There are several types of porous materials, including cellular, fibrous and granular, and some examples are porous polymers, mineral fibres and porous concrete [1]. Porous concrete containing light aggregates, with an adequate amount of air, has excellent characteristics, including good workability, low density and proper strength, and can be applied in architectural elements with good acoustic and thermal behaviour [2]. This type of material has been used in numerous applications, such as outside noise barriers near roads and railways, to improve this kind of mitigation measure. It is composed of a solid and a fluid part, and the sound energy dissipation occurs due to the interaction between these two phases [1, 3]. To study porous materials, several approaches can be used, namely experimental and theoretical. Using the impedance tube to study the sound absorption coefficient with normal sound incidence, described in ISO 10534-2 [4], is a non-expensive and easy to do option that can provide interesting results. Nevertheless, it has some debilities because, in the real context, it is usual to have diverse sound incident angles instead. However, this method also gives the values for the surface impedance of the material. To experimentally determine the sound absorption coefficient of a material sample in diffuse field conditions, the procedure proposed by ISO 354 [5] could be used. This experimental procedure has the advantage of considering multiple sound incident angles and use a larger sample, and can be found more realistic, but it is indeed more expensive than the previous procedure. In order to get values of sound absorption in diffuse field conditions based on values obtained with plane waves, different theoretical approaches were suggested by some authors. The ISO 10534-2 [4], based on London's equations and also London's equations [6], make the transformation from the sound absorption coefficient with normal incidence, obtained with an impedance tube, to diffuse field

conditions. In this case, the medium is considered as infinite, and the propagation inside the medium is locally reactive.
Fluid-equivalent models have been presented considering the complex bulk modulus and fluid-equivalent density to represent the absorbing behaviour of the porous materials studied [3, 7-11]. In this work, the model proposed by Horoshenkov-Swift [7] has been used to compute the sound absorption from the measured macroscopic parameters. This model represents the behaviour of the porous samples based on four parameters: air-flow resistivity, tortuosity, open porosity, and the standard deviation of the pore size, of which the first three have been determined both experimentally and by an inverse method, while the last on was estimated only by inversion techniques [12].
The structure of the paper is as follows: Section 2 – Materials, introduces the samples physical characteristics (e. g., grain size, ratio aggregate/cement); in Section 3 - Methodology, the used methodology is presented, along with a brief explanation of the experimental methods and theoretical models; in Section 4 – Results and discussion, results concerning the sound absorption coefficient determined by different methods are presented and analysed; and finally, Section 5 – Conclusions, describes the main conclusion of this study.

2 Materials

In this work, the aggregate used in the porous concrete mixtures was expanded clay. Tests were carried out for normal sound incidence in an impedance tube and in diffuse field conditions in a reverberation room to obtain the samples sound absorption coefficient.

For the expanded clay in Figure 1, the grain size was obtained by cutting the material and has a grain size distribution in a range of approximately 0.25 to 3.15 mm (Figure 2).

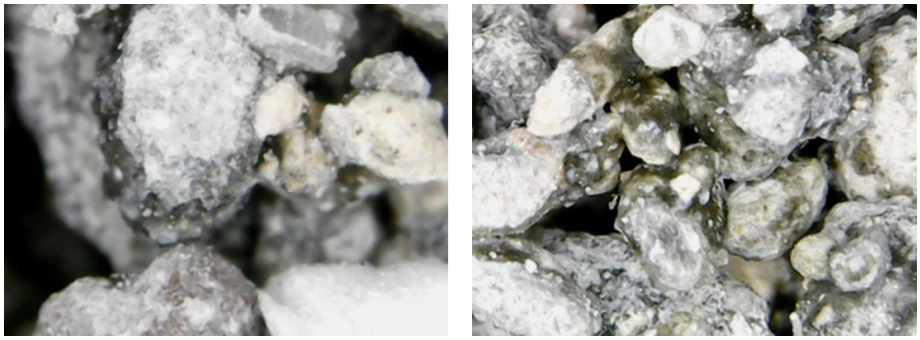

Figure 1 – Expanded clay used.

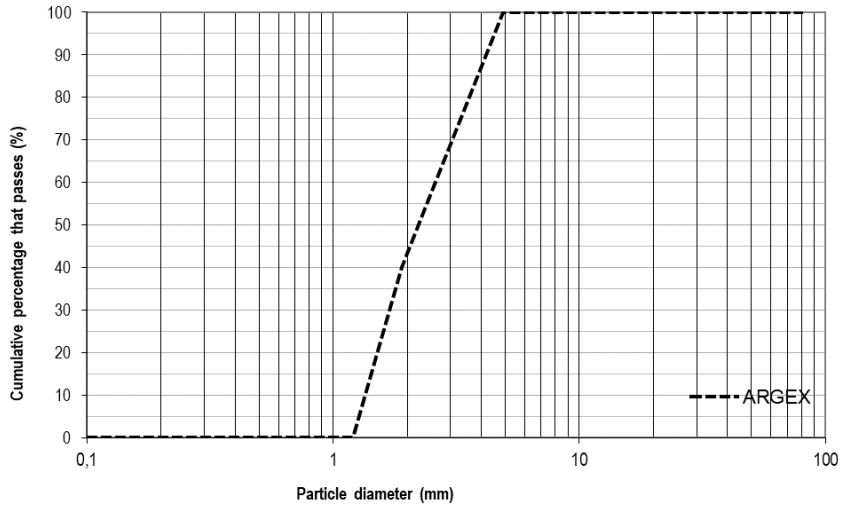

Figure 2 – Grain size distribution obtained using the procedure described in EN 993-1:1997 [13].

For the tests carried out in impedance tube, concrete cement-based mixtures were prepared, with this expanded clay, in circular moulds about 10 cm in diameter and thickness of 4 and 8 cm (Figure 3).

Figure 3 – Porous concrete samples, for impedance tube.

Three different aggregate/cement ratios, (A/C) were prepared, with expanded clay, and 6 samples for each mixture were obtained, of which 3 for each sample thickness (Table 1). From now on, they are referred by their trade names and aggregate/cement ratios.

Table 1 – Mixtures prepared of lightweight porous concrete.

Expanded Clay	A/C	Mass percentage [%]		
		Cement	Aggregate	Water
Argex/AE	2.93	20.40	59.78	19.81
Argex/AE	3.71	17.51	64.97	17.51
Argex/AE	5.18	13.93	72.14	13.93

A preliminary study was conducted to perceive the moisture influence in the sound absorption coefficient measures on the impedance tube. The measures were made at 7, 14 and 28 days after the sample was prepared. It showed only slight differences between curves of the same samples, thus seeming not to have a very strong influence. These results are consistent with those shown by Ramis et al [14].

For the tests carried out in the reverberant room, in diffuse field conditions, two porous concrete samples were tested, with an approximate area of 10 m^2 (Figure 4) and the porous layer with approximate 8 cm.

Figure 4 – Porous concrete samples, for reverberant chamber.

3 Methodology

Several experimental tests and theoretical models were used in this work to compare the behaviour of porous concrete made with expanded clay. The main objective of this work is to compare the results obtained with different strategies for cement-based porous materials.

3.1 Experimental Procedures

3.1.1 Sound absorption coefficient – normal incidence

To find sound absorption coefficient with normal incidence, tests were performed on a circular impedance tube with 100 mm diameter. The test methodology used is proposed in ISO 10534-2-2 [4], which is based on the transfer function between two microphones.

The impedance tube used has a cut-off frequency of about 1600 Hz. The sound pressure was measured using two G.R.A.S. Sound & Vibration 46 AE 1/2" CCP free field microphones, a NI USB 4431 acquisition system, (National Instruments) and the pressure data processed in MATLAB. A random excitation provided by a speaker was generated from the NI USB 4431.

The ratio between the reflected pressure (p_r) and the incident pressure (p_i) is the reflection factor that is given by equation (1):

$$r = \frac{p_r}{p_i}. \tag{1}$$

The sound absorption coefficient can be achieved with equation (2):

$$\alpha = 1 - |r|^2, \tag{2}$$

where r is the reflection coefficient. This experimental test also provides an important parameter that characterises acoustically the material, the surface impedance (3):

$$Z_{sf} = \rho_0 c_0 \frac{(1+r)}{(1-r)}, \tag{3}$$

where $\rho_0 c_0 = Z_0$ is the characteristic air impedance.

3.1.2 Sound absorption coefficient – diffuse field

To determine the sound absorption coefficient in diffuse field conditions, tests were performed in a reverberant room. This test methodology is proposed in ISO 354 [5]. The diffuse incidence absorption coefficient measurement procedure consists of making room reverberation time (T60) measurements under two distinct conditions. In the first measurement, the reverberant room is empty, and in the second, the sample to be characterized is positioned, and the second measurement of T60 is taken. The sample equivalent absorption area can be achieved with expression (4):

$$A_T = A_2 - A_1 = 55{,}3V\left(\frac{1}{c_2 T_2} - \frac{1}{c_1 T_1}\right) - 4V(m_2 - m_1), \tag{4}$$

where V is the volume of the empty reverberant room, c_1 is the propagation speed of sound in air at temperature t_1 with the empty room, m_1 is the attenuation coefficient due to the presence of air with the empty room, T_1 is the reverberation time of the room empty, c_2 is the sound propagation velocity in air at temperature t_2 with the sample in the room, m_2 is the attenuation coefficient due to the presence of air with the sample in the room and T_2 is the reverberation time with the sample in the room.

The sound absorption coefficient, in diffuse field conditions, must be calculated according to expression (5):

$$\alpha_s = \frac{A_T}{S}, \tag{5}$$

in which S is the sample area.

3.2 Theoretical Models

Porous materials are made up of two phases, solid and fluid, making it possible to predict their behaviour in numerical models as equivalent fluids [3, 7, 8, 15] . The Horoshenkov and Swift model for granular porous materials was used, adequate for porous concrete samples, such as those studied. The model allows estimating the acoustic behaviour from the macroscopic properties of the material. From these parameters and considering the porous material to behave like an equivalent fluid, it is possible to determine the characteristic impedance and the wavenumber of the material. The parameters considered were the porosity, ϕ, the airflow resistivity, σ, the tortuosity, α_∞, and the standard deviation of the pore size, σp, of which the first three have been determined both experimentally ([16-18]) and by an inverse method (Table 2). In contrast, the last one was determined only theoretically. These authors suggest to determine the volumetric density and the compressibility module with equations (6) and (7), respectively:

$$\rho = \frac{\alpha_\infty}{\phi}\left(\rho_0 - \frac{j\phi\sigma}{\omega\alpha_\infty}\tilde{F}(\omega)\right) \tag{6}$$

$$C = \frac{\phi}{\gamma P_0}\left(\gamma - \frac{\rho_0(\gamma-1)}{\rho_0 - j\frac{\sigma\phi}{\omega\alpha_\infty N_{pr}}\tilde{F}(N_{pr}\omega)}\right), \tag{7}$$

where: ω is the angular frequency, γ is the ratio of specific heat, P_0 is the atmospheric pressure and N_{pr} is the number of Prandtl number and $\tilde{F}$ is the viscosity correction function, which can be presented in the form of a Padé approximation as in (8):

$$\tilde{F}(\omega) = \frac{1 + a_1\epsilon + a_2\epsilon^2}{1 + b_1\epsilon}. \tag{8}$$

With these two parameters, it is possible to obtain the characteristic impedance and the wave number of a porous material. Which are determined according to equations (9) and (10):

$$Z_c = \sqrt{\rho/C} \tag{9}$$

$$k = \omega\sqrt{\rho C}, \tag{10}$$

where: $a_1 = \theta_1/\theta_2$, $a_2 = \theta_1$ and $b_1 = a_1$. Assuming in a simplified way that the geometry of the pores is circular, thus leads to the following form factors: $\theta_1 = \frac{4}{3}e^{4\xi} - 1$, $\theta_2 = \frac{e^{3\xi/2}}{\sqrt{2}}$, where $\xi = \left(\sigma_p \ln(2)\right)^2$ and $\epsilon = \sqrt{j\omega\rho_0\alpha_\infty/(\sigma\phi)}$.

An inverse method was also used based on a genetic algorithm to determine the macroscopic parameters theoretically and obtained a new sound absorption curve. This method is based on the difference between the theoretical sound absorption coefficient obtained with the Horoshenkov and Swift model and the experimental sound absorption coefficient. For the use of this inversion algorithm, an initial estimation (based on the experimental results) and lower and upper boundary limits were defined for each macroscopic parameter. Such process ensures that the values obtained are within acceptable values. The following objective function (11) is then minimized:

$$Fu = \sum_{i=1}^{nf} |\alpha_s^a - \alpha_s^e|^2 \tag{11}$$

where: nf is the number of discrete frequencies analysed, α_s^a is the absorption coefficient obtained with Horoshenkov and Swift model and α_s^e is the experimental absorption coefficient. The experimental and corrected macroscopic parameters for both considered thickness, 8 and 4 cm, are presented in Table 2. These values represent the average value of each type of mixture and thickness.

Table 2 – Experimental and corrected (theoretical) macroscopic parameters.

Sample	Thickness [m]	Tortuosity α_∞ [-]	Porosity Φ [-]	Airflow resistivity σ [Ns/m4]	Average pore size standard deviation σ_p [-]
Experimental data					
Argex/AE 2.93	0.08	2.51	0.46	4507.88	0.25
	0.04	3.81	0.42	6246.85	0.25
Argex/AE 3.71	0.08	2.21	0.45	5044.94	0.25
	0.04	3.50	0.42	6045.70	0.25
Argex/AE 5.18	0.08	2.37	0.46	4668.45	0.25
	0.04	3.80	0.45	5324.50	0.25
Theoretical data					
Argex/AE 2.93	0.08	2.26	0.45	4720.11	0.26
	0.04	3.43	0.46	6871.49	0.27
Argex/AE 3.71	0.08	2.14	0.45	5231.79	0.27
	0.04	3.15	0.46	6642.98	0.27
Argex/AE 5.18	0.08	2.14	0.50	4990.16	0.27
	0.04	3.42	0.50	5738.34	0.27

Theoretical models exist to make the transformation from experimental results of sound absorption coefficient with normal incidence to diffuse field conditions, using several simplifications. In ISO 10534-2 [4], one of the equations proposed by London, equation (12), is presented:

$$\alpha_d = 8\gamma_n \left[1 - \gamma_n ln\left(\frac{r'}{\gamma_n} + 2r' + 1\right) + \left(\frac{x'}{r'}\right)\gamma_n \left(\left(\frac{r'}{x'}\right)^2 - 1\right) arctan\left(\frac{x'}{r'+1}\right)\right], \tag{12}$$

where $\gamma_n = r'/(r'^2 + x'^2)$, $r' = Re(\tilde{Z}_{exp}/\rho_0 c_0)$, $x' = Im(\tilde{Z}_{exp}/\rho_0 c_0)$, and $\tilde{Z}_{exp}$ is the surface impedance obtained experimentally. The so-called first and second London equations are also presented by expressions (13) and (14):

$$\alpha_b = 8\left[\frac{1-\sqrt{1-\alpha_n}}{1+\sqrt{1-\alpha_n}}\right]^2\left[\left(\frac{2}{1-\sqrt{1-\alpha_n}}\right)-\frac{1-\sqrt{1-\alpha_n}}{2}+2ln\left(\frac{1-\sqrt{1-\alpha_n}}{2}\right)\right] \quad (13)$$

$$\alpha_s = 4\left[\frac{1-\sqrt{1-\alpha_n}}{1+\sqrt{1-\alpha_n}}\right]\left[ln\left(\frac{2}{1-\sqrt{1-\alpha_n}}\right)-\frac{1+\sqrt{1-\alpha_n}}{2}\right]. \quad (14)$$

4 Results and discussion

The results of the developed work are presented and analysed. First, the results obtained by directly measuring the sound absorption coefficient in the impedance tube are shown, and in the following section, the sound absorption coefficient results for diffuse field conditions, both experimental and theoretical, are presented.

4.1 Normal incidence

The experimental and theoretical sound absorption coefficient curves with incident plane waves are presented in Figure 5. The experimental results were obtained according to ISO 10534-2 [4]. The theoretical curves were obtained with the proposed model of Horoshenkov and Swift, where experimental macroscopic parameters (PMe) and corrected macroscopic parameters (PMc) were used.

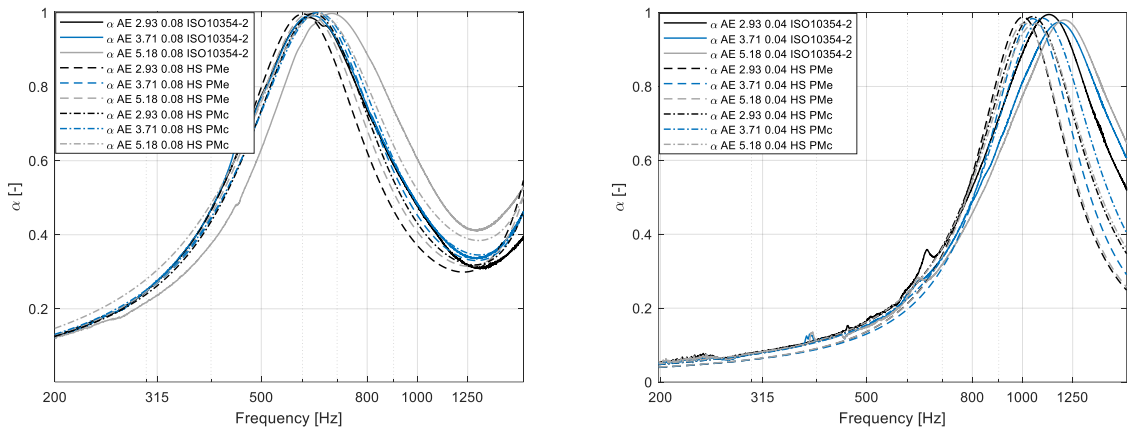

(a) (b)

Figure 5 – Experimental and theoretical sound absorbent curves, for normal incidence waves, for 8 cm (a) and 4 cm (b) samples.

Both theoretical curves fit quite well to the experimental data. It must be noticed that the adjustment between corresponding curves is better for samples with 8 cm thickness than to 4 cm thickness. However, it can be observed that the curves obtained with the corrected macroscopic parameters obtained with the previously introduced inverse method adjust slightly better than the ones with experimental macroscopic parameters.
The samples present very similar behaviours because despites the different aggregate/cement ratios, the differences between each other are only slight. Appreciable sound absorption can be observed between 400 and 1000 Hz for the 8 cm samples and 800 and 1600 Hz for the 4 cm samples. The maximum amplitude is observed between 600 and 700 Hz for the 8 cm samples and 1000 and 1250 Hz for the 4 cm samples.

For each mixture, the displacement of the absorption curve to higher frequencies is observed with the decrease in thickness, as it was expected.
For different mixtures and the same thickness, it can be observed that the sound absorption curve moves to lower frequencies for a greater amount of cement. With cement's increase, the density of the sample also increases (presenting smaller pores/channels), thus changing some of the macroscopic parameters that influence the acoustic behaviour.

4.2 Diffuse field conditions

The experimental and theoretical sound absorption coefficient curves in diffuse field conditions are presented in Figure 6 for the mixture Argex/AE 5.18. For all cases, the experimental and theoretical simulation were obtained for a thickness of 8 cm.

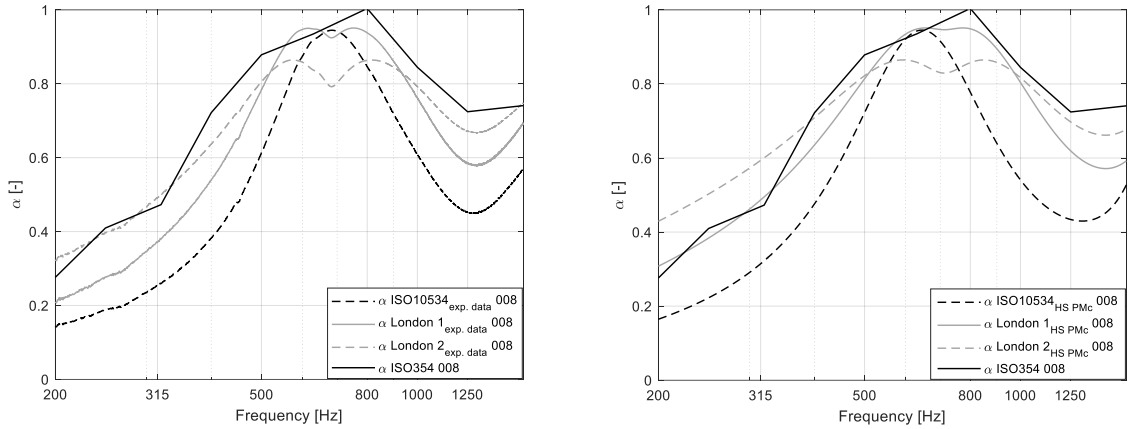

(a) (b)

Figure 6 – Experimental and theoretical sound absorption curves in diffuse field conditions, considering the directly measured normal incidence sound absorption (a), and for Horoshenkov and Swift model with corrected macroscopic parameters (b).

Comparing the sound absorption curves obtained for both conditions, results for normal incident waves and for diffuse field conditions reveal quite different behaviours. As expected, a wider frequency range with higher sound absorption coefficient is seen for the diffuse field, clearly revealing the effect of refracted sound waves within the material volume.
Analysing the different approaches for the estimation of diffuse field absorption, the curve obtained by the equation suggested in ISO 10534-2 [5] (α ISO10534-2 $_{exp.data}$ 008) presents significant differences when compared with the experimental curve measured in a reverberant room (α ISO354 008).
On the other hand, London's equation 1 (α London 1 $_{exp.data}$ 008 and α London 1 $_{HS\ PMc}$ 008) seems to adjust better to the experimental curve, especially the one obtained with the Horoshenkov and Swift model and the corrected macroscopic parameters of the studied material. The second London equation also leads to similar results, but seems to estimate higher values at lower frequencies, and lower absorptions in the mid-frequency range. It should be noted that the calculated diffuse field absorption resulting both from ISO 10534-2 and from London's equations is an approximate estimation which should only be valid when locally reacting materials are analysed. In the present case, the tested solution is clearly bulk-reacting, and so significant deviations occur. Additionally, all equations refer to infinite panels, while the diffuse field test was performed for a finite 3x3 m^2 panel, which induces a different behaviour of the whole solution (see [19]).
One final plot is presented in Figure 7, depicting the comparison between the measured sound absorption in the reverberant room with the two London models, considering 1/3 octave bands, and the complete frequency range between 125 Hz and 4000 Hz. Observing these curves, it can be seen that the global trend is correctly predicted by the two simplified models, although with some discrepancies and oscillations being

visible. Even in the higher frequency range above 2000 Hz (which was not measured in the impedance tube), the global trend seems to be followed by the predictions based in the Horoshenkov and Swift theoretical model together with the London models.

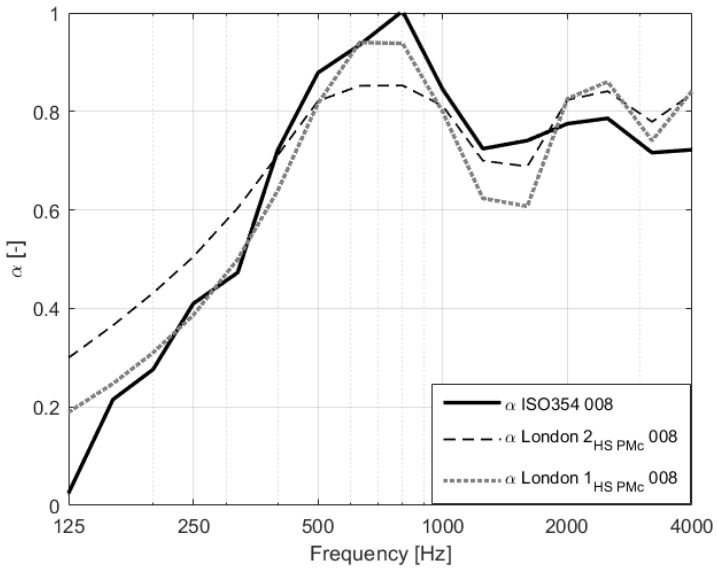

Figure 7 – Experimental and theoretical sound absorption curves in diffuse field, in 1/3 octave bands, for both London models.

5 Conclusions

Different approaches can be used to study the acoustic behaviour of porous materials. This work intends to study sound absorption provided by porous cement-based materials and evaluate different estimating strategies. Different experimental and theoretical models were used.

Several porous concrete samples, composed of expanded clay, cement and water, were tested. These revealed the expected sound absorption behaviour, with a structure of peaks and valleys which is related to the specimen thickness and to its macroscopic parameters.

A theoretical model proposed by Horoshenkov and Swift proved to be efficient to predict the sound absorption behaviour, when subject to plane waves, of this type of material. The inverse method used to obtain the corrected macroscopic parameters enables the Horoshenkov and Swift curves to adjust better to the experimental curves.

For the diffuse field conditions analyses, all tested models seem to provided only a rough approximation of the sound absorption curve, with clear differences being registered between both the simplified and the measured results. Indeed, this is a complex problem, and the bulk reactive character of the solution together with its finite size and with possible internal heterogeneities within the material lead to the necessity of better estimation tools. Numerical tools, based on the BEM or FEM may be an option to perform more accurate estimation.

Acknowledgements

This work was partly financed by FCT – Fundação para a Ciência e a Tecnologia, I.P., within the scope of the research unit “Institute for sustainability and innovation in structural engineering - ISISE” (UIDP/04029/2020), and by the FEDER funds through COMPETE 2020, Portugal 2020, under the project POCI-01-0247-FEDER-033990 (iNBRail). Acknowledgements to persons or institutions should be placed in this section.

FCT Fundação para a Ciência e a Tecnologia
MINISTÉRIO DA CIÊNCIA, TECNOLOGIA E ENSINO SUPERIOR

References

[1] Fahy, F. J. *Foundations of engineering acoustics,* Academic Press, Southampton (United Kingdom), 1st Edition, 2000.
[2] Kim, H.-K.; Jeon, J. H.; Lee, H.-K. Workability, and mechanical, acoustic and thermal properties of lightweight aggregate concrete with a high volume of entrained air, *Construction Building Materials,* Vol 29, 2012, pp 193-200.
[3] Cox, T.; d'Antonio, P. *Acoustic absorbers and diffusers: theory, design and application,* Crc Press, New York (United States of America), 2nd Edition, 2016.
[4] ISO, International Organization for Standardization. ISO 10534-2: *Acoustics — Determination of sound absorption coefficient and impedance in impedance tubes - Part 2: Transfer-function method,* Genève, 1998.
[5] ISO, International Organization for Standardization. ISO 354: *Acoustics - Measurement of sound absorption in a reverberation room,* Genève, 2003.
[6] London, A. The determination of reverberant sound absorption coefficients from acoustic impedance measurements, *The Journal of the Acoustical Society of America,* Vol 22 (2), 1950, pp 263-269.
[7] Horoshenkov, K. V.; Swift, M. J. The acoustic properties of granular materials with pore size distribution close to log-normal, *The Journal of the Acoustical Society of America*, Vol 110 (5), 2001, pp 2371-2378.
[8] Allard, J.; Atalla, N. *Propagation of sound in porous media: modelling sound absorbing materials,* John Wiley & Sons, Chichester (United Kingdom), 2nd Edition, 2009.
[9] Allard, J.-F.; Champoux, Y. New empirical equations for sound propagation in rigid frame fibrous materials, *The Journal of the Acoustical Society of America*, Vol 91 (6), 1992, pp 3346-3353.
[10] Panneton, R. Comments on the limp frame equivalent fluid model for porous media, *The Journal of the Acoustical Society of America,* Vol 122 (6), 2007, pp EL217-EL222.
[11] Champoux, Y.; Allard, J.-F. Dynamic tortuosity and bulk modulus in air-saturated porous media, *Journal of Applied Physics,* Vol 70 (4), 1991, 1975-1979.
[12] Lourenço de Sousa, L.; Pereira, L.; Godinho, L.; Mendes, P. A., editors. Acoustic properties of porous concrete-Experiments and modelling, *INTER-NOISE and NOISE-CON Congress and Conference Proceedings 2020,* Seul, Korea, August 23-26, 2020, Vol 261 No 6, pp 127-137, Institute of Noise Control Engineering.
[13] CEN, European Standard EN 993-1: *Tests for geometrical properties of aggregates - Part 1: Determination of particle size distribution — Sieving method,* Belgium, 1997.
[14] Ramis, E.; Pereira, M.; Branco, F. G.; Godinho, L.; Amado, P. An experimental study of the influence of moisture content in acoustic absorption of porous concrete, *Tecniacústica 2018*, Cádiz, Spain,October 24-26, 2018, In CD-ROM.
[15] Panneton, R.; Atalla, N. Numerical prediction of sound transmission through finite multilayer systems with poroelastic materials, *The Journal of the Acoustical Society of America,* Vol 100 (1), 1996, pp 346-354.
[16] CEN, European Standard EN 1936: *Natural stone test methods - Determination of real density and apparent density, and of total and open porosity,* Belgium, 2007.
[17] ISO, International Organization for Standardization. ISO 9053: *Acoustics - Materials for acoustical applications - Determination of airflow resistance,* Genève, 1991.
[18] Mafra, M. P. A. Desenvolvimento de bancada experimental e determinação da tortuosidade de materiais poroelásticos, utilizando o método da condutividade elétrica, *XII Congresso nacional de estudantes de engenharia mecânica 2005,* São Paulo, Brasil, August 22-26, 2005.
[19] Pereira, M.; Mareze, P. H.; Godinho, L.; Amado-Mendes, P.; Ramis, J. Proposal of numerical models to predict the diffuse field sound absorption of finite sized porous materials – BEM and FEM approaches, *Applied Acoustics*, Vol 180, 2021, pp 108092.